



Received: 2026.03.17

Accepted: 2026.06.22

Available online: 2026.07.07

Published: 2026.XX.XX

# Retrospective Cohort Study Comparing Digitally Customized 3D-Printed Partial Talus Replacement and Ankle Arthrodesis for Extensive Talus Necrosis: Early Clinical Outcomes

Authors' Contribution:  
Study Design A  
Data Collection B  
Statistical Analysis C  
Data Interpretation D  
Manuscript Preparation E  
Literature Search F  
Funds Collection G

AEG 1,2 **Heda Liu**  
BF 1 **Pengwei Li**  
BC 1 **Fei Huang**  
C 1 **Lin Liu**  
C 1 **Sheng Liu**  
A 2 **Ming Li**

1 Department of 1st Foot and Ankle Surgery, Cangzhou Hospital of Integrated TCM-WM Hebei, Cangzhou, Hebei, PR China  
2 Hebei Key Laboratory of Integrated Traditional and Western Medicine in Osteoarthritis Research, Cangzhou, Hebei, PR China

**Corresponding Author:** Ming Li, No.31 West Huanghe Road, Cangzhou 061001, Hebei, China, Phone: +86 17331788600, Fax: +86 317 2135800, e-mail: [drliming1@163.com](mailto:drliming1@163.com)  
**Financial support:** This study was supported by the Science and Technology Bureau of Cangzhou (grant No. 23244102169)  
**Conflict of interest:** None declared

**Background:** This retrospective study from a single center included 105 patients with avascular necrosis of the talus in our hospital from January 2021 to January 2024 and aimed to compare outcomes from management with customized 3-dimensional (3D) printed partial talus replacement with ankle arthrodesis.

**Material/Methods:** The replacement group (n = 49) received digital customized 3D-printed partial talus replacement surgery, and the arthrodesis group (n = 53) underwent ankle arthrodesis. Efficacy of the 2 surgical methods was evaluated by comparing the American Orthopaedic Foot and Ankle Society (AOFAS) ankle-hindfoot score, pain visual analog scale (VAS), ankle range of motion (ROM), SF-36 quality of life scale, and complication rate before surgery and at last follow-up.

**Results:** At final follow-up, the observation group showed significantly better outcomes than the conventional group in AOFAS score ( $85.88 \pm 3.56$  vs  $78.51 \pm 4.12$ ,  $P < 0.001$ ), ankle ROM ( $48.31^\circ \pm 4.95^\circ$  vs  $0.91^\circ \pm 1.13^\circ$ ,  $P < 0.001$ ), and the SF-36 Physical Component Summary ( $74.12 \pm 4.10$  vs  $55.83 \pm 4.96$ ,  $P < 0.001$ ) and Mental Component Summary ( $81.26 \pm 5.12$  vs  $68.15 \pm 5.93$ ,  $P < 0.001$ ). VAS scores were also significantly lower in the observation group ( $1.71 \pm 0.71$  vs  $2.57 \pm 0.87$ ,  $P < 0.001$ ). Overall complication rates were similar (8.1% vs 11.3%,  $P = 0.592$ ); however, the reoperation rate was lower in the observation group (0% vs 3.7%).

**Conclusions:** In early follow-up, 3D-printed partial talus replacement for extensive talus necrosis demonstrates superior joint function, ROM, and quality of life compared with ankle arthrodesis, without increasing complications, suggesting it is a safe and effective joint-preserving alternative.

**Keywords:** Arthrodesis • Printing, Three-Dimensional • Talus

Full-text PDF: <https://www.medscimonit.com/abstract/index/idArt/953450>

3422

4

4

31



Publisher's note: All claims expressed in this article are solely those of the authors and do not necessarily represent those of their affiliated organizations, or those of the publisher, the editors and the reviewers. Any product that may be evaluated in this article, or claim that may be made by its manufacturer, is not guaranteed or endorsed by the publisher

## Introduction

Avascular necrosis of the talus is a progressive and debilitating condition resulting from compromised blood supply to the talus. Avascular necrosis of the talus is commonly associated with trauma, corticosteroid use, chronic alcohol consumption, or idiopathic etiologies [1,2]. The underlying pathophysiology involves osteonecrosis, subsequent structural collapse of the talus, and the development of secondary ankle osteoarthritis due to impaired vascular perfusion [3]. Diagnosis is primarily based on imaging, with magnetic resonance imaging (MRI) being the gold standard for early detection and for assessing the extent of necrosis, while computed tomography (CT) is crucial for evaluating bone collapse and cortical involvement [4]. Clinically, patients typically present with severe pain, marked functional impairment, and a substantial reduction in quality of life, making avascular necrosis of the talus a challenging entity in the field of foot and ankle surgery [5,6].

For extensive talar necrosis, typically defined as a necrotic area involving more than 50% of the talar volume or a collapse depth exceeding 2 mm, conventional treatment approaches present significant challenges. Conservative management is generally ineffective, while surgical options remain limited. Although ankle arthrodesis can effectively alleviate pain, it compromises all joint mobility and adversely affects gait mechanics and function of adjacent joints [7]. Total ankle arthroplasty is associated with concerns regarding implant longevity, high wear rates, and elevated revision rates, making it particularly unsuitable for young, active patients [8]. Vascularized pedicled bone grafting entails risks such as donor site morbidity, graft resorption, and technical difficulties in contouring; studies indicate that approximately 35% of patients experience donor site discomfort [9,10]. Consequently, there is a pressing need for a novel therapeutic approach that preserves joint function, restores anatomical integrity, and ensures long-term stability.

In recent years, the rapid advancement of digital design and additive manufacturing (3-dimensional [3D] printing) technologies has opened new avenues for addressing this challenge [11,12]. Digital customized 3D-printed partial talar replacement has emerged as a promising solution. This approach involves mirror reconstruction of CT and MRI data from the patient's healthy ankle joint or precise segmentation of the non-necrotic regions on the affected side, enabling the personalized design and fabrication of bioporous prostheses that closely match the patient's anatomical structure. The porous architecture of the prosthesis is specifically engineered to facilitate bone ingrowth and achieve biological fixation, thereby restoring the normal biomechanical function of the ankle joint [13-15].

Although digitally customized 3D-printed partial talus replacement has demonstrated considerable potential, systematic evaluation

of its efficacy remains lacking. To address this gap, the present study designed a retrospective cohort analysis to systematically assess the early clinical efficacy and safety of this innovative surgical technique. Therefore, this retrospective study from a single center included 105 patients with avascular necrosis of the talus and aimed to compare outcomes from management with customized 3D-printed partial talus replacement with ankle arthrodesis evaluated using the American Orthopaedic Foot and Ankle Society (AOFAS) ankle-hindfoot score, the pain visual analog scale (VAS), ankle range of motion (ROM), the 36-Item Short Form Health Survey (SF-36), and postoperative complication rates.

## Material and Methods

### Ethics Statement

The study was approved by the Ethics Committee of Cangzhou Integrated Traditional Chinese and Western Medicine Hospital of Hebei Province (CZX2024191-1) and the requirement for informed consent was waived by the Ethics Committee of our hospital since this was a retrospective study and the data were anonymous.

### Inclusion and Exclusion Criteria

This study retrospectively analyzed the clinical data of 105 patients with massive talar necrosis who received treatment in our department between January 2021 and January 2024. Based on the differing treatment modalities, the patients were categorized into the arthrodesis group, which underwent ankle arthrodesis, and the replacement group, which received 3D-printed partial talar replacement. The inclusion criteria were as follows: (1) age between 18 and 65 years; (2) confirmation of extensive unilateral talus necrosis via imaging modalities (X-ray, CT, or MRI), defined as necrotic involvement of 30% or more of the talar volume or affecting the primary weight-bearing region; (3) persistent and clinically significant ankle pain with functional impairment refractory to standard conservative management for more than 6 months; and (4) availability of complete clinical records. Exclusion criteria were as follows: (1) total talus necrosis; (2) history of prior ipsilateral ankle surgery; (3) presence of severe ankle osteoarthritis or other significant foot joint pathology; (4) uncorrected severe lower limb malalignment (varus or valgus deformity exceeding 10°); (5) severe neurovascular disease or compromised soft tissue integrity; (6) active local ankle infection or systemic infection; and (7) severe medical comorbidities contraindicating surgical intervention.

### Preoperative Management

Patients routinely received X-ray, CT, MRI and other imaging examinations of the ankle joint (**Figure 1**). A 64-slice spiral

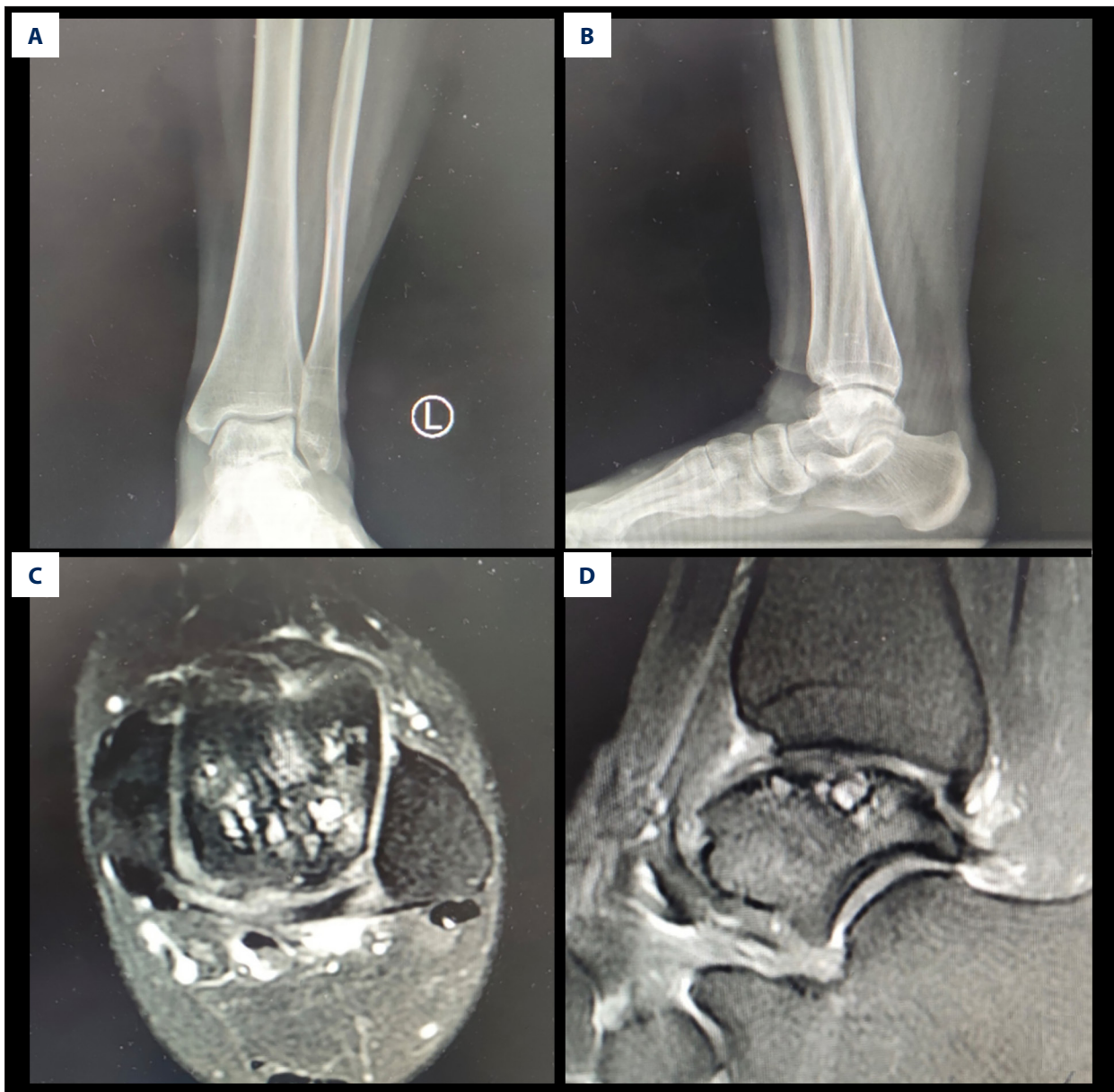


**Figure 1.** A 40-year-old female patient presented with massive necrosis of the left talus. Preoperative weight-bearing anteroposterior (A) and lateral (B) radiographs suggested necrosis of the left talus. MRI (C, D) demonstrated multiple cystic changes beneath the articular surface of the left talus.

CT scanner (Somatom Definition AS, Siemens Healthineers, Erlangen, Germany) was used to evaluate the size and stability of the bone cyst wall, and MRI (Magnetom Skyra, Siemens Healthineers) was used to determine the stability of the talar cartilage and the extent of the lesion [16]. At the same time, the ankle dorsiflexion, plantarflexion, adduction, and abduction ROM were measured, and the lower limb alignment, bone condition, and medial and lateral ligament stability were evaluated.

The ankle CT thin-section scan data (slice thickness: 0.625 mm) were imported into Mimics 21.0 software (Materialise

NV, Leuven, Belgium). Based on the size and location of the bone defect identified in the CT images, 3D reconstruction of the talus was performed using the software to accurately delineate the lesion area and reconstruct the defect model (Figure 2A, 2B). Using this reconstructed model, a personalized talus prosthesis and a corresponding osteotomy guide plate were designed (Figure 2C). The design considered the optimal screw trajectory and incorporated a porous structure (average pore size 600  $\mu\text{m}$ , porosity 70%) to facilitate bone ingrowth. Subsequently, the osteotomy guide plate model and the solid model derived from the ankle joint CT reconstruction were

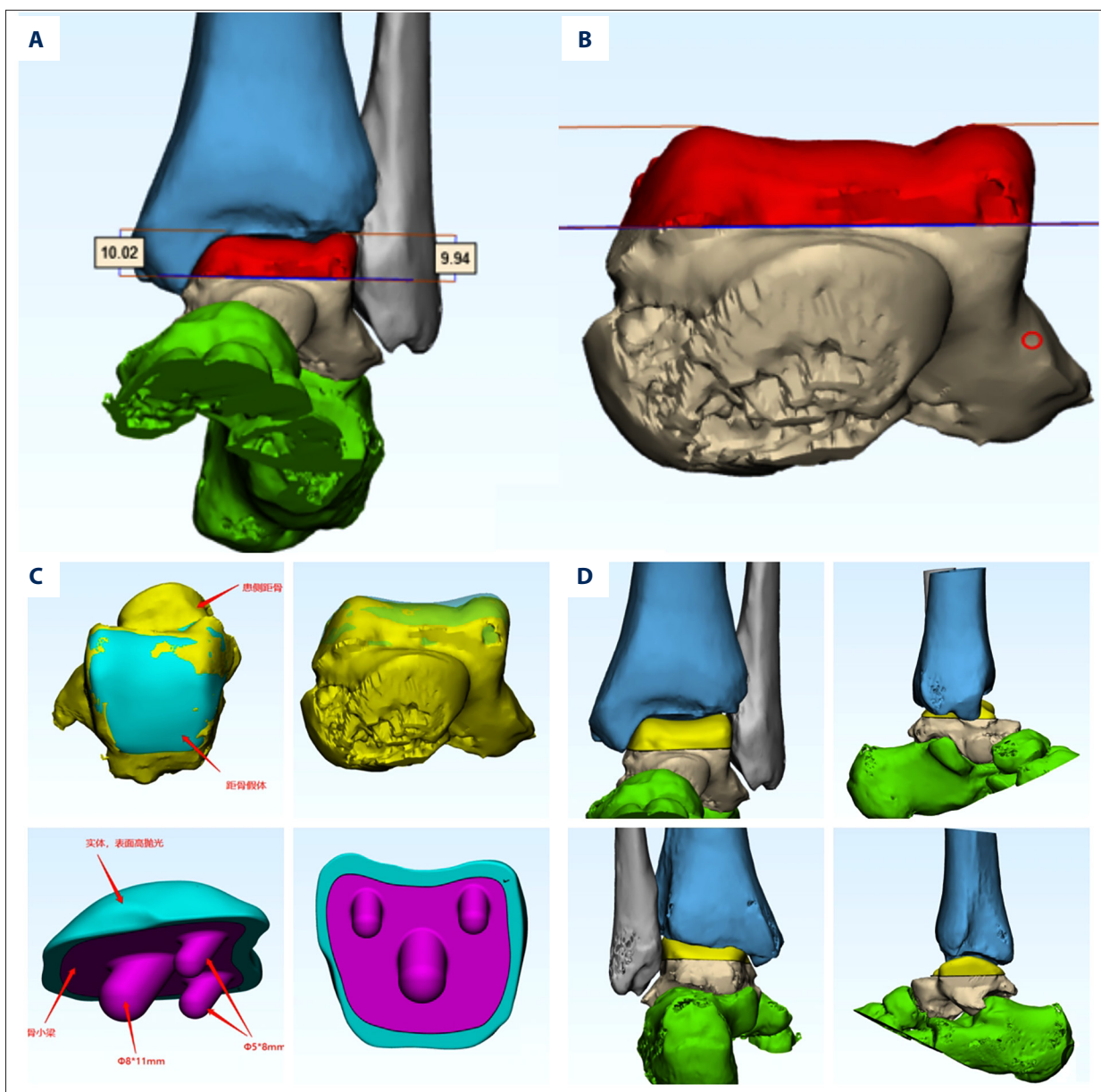


**Figure 2.** The operative plan was developed based on preoperative 3D simulation. (A, B) The red area indicates the bone to be excised. (C) The custom talus prosthesis designed using 3D printing technology. (D) The preassembly plan of the prosthesis, indicating the planned intraoperative position of the talar prosthesis.

integrated into the overall 3D lower limb model for simulated surgical validation (Figure 2D). The finalized 3D model of the osteotomy guide plate was then transferred to our hospital's 3D printing center, where it was printed using photosensitive resin (Somos WaterShed XC 11122, DSM, The Netherlands) via a stereolithography printer (ProX 950, 3D Systems, Rock Hill, SC, USA), followed by sterilization, sealing, and packaging for clinical use. Concurrently, the custom partial talus prosthesis was fabricated via metal 3D-printing technology (Shanghai Kuanyue Xinchengshi Medical Technology Co, Ltd).

### Surgical Procedure

All procedures were conducted with patients under spinal anesthesia, with a tourniquet applied in each case. Prophylactic antibiotics were administered routinely 30 minutes prior to surgery to minimize the risk of infection.

In the arthrodesis group, ankle arthrodesis was conducted using the following procedure. A longitudinal incision approximately 8 to 12 cm in length was made using the anterior ankle approach. The skin and subcutaneous tissue were cut in

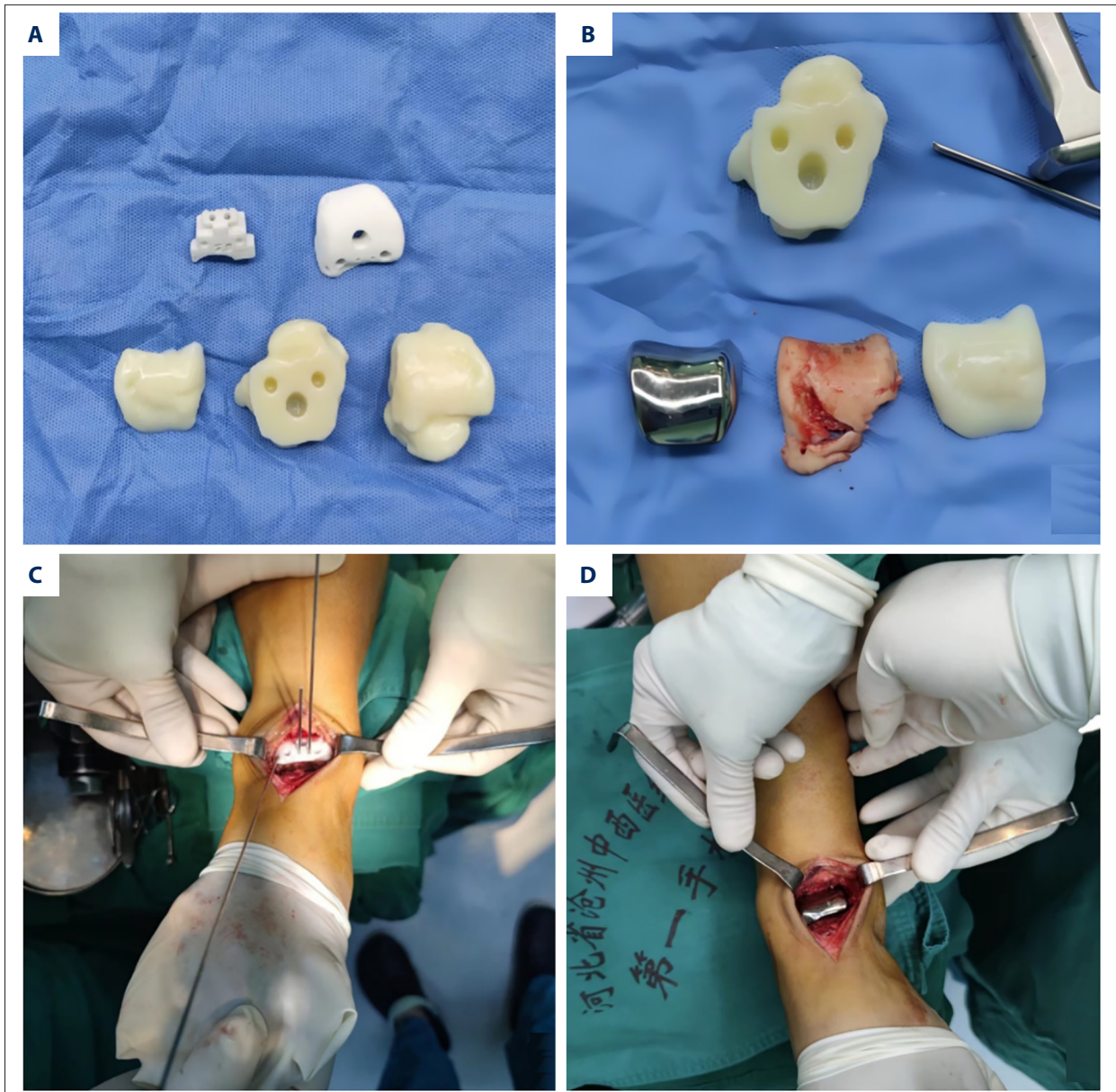


**Figure 3.** (A) The 3D-printed talus solid model and the supporting navigation template based on the patient's CT data. (B) Comparison of the talus after resection of the diseased bone with the preoperative model to verify the accuracy of the osteotomy range. (C) Installation and fixation of the talus surface model under the precise guidance of the navigation template. (D) Implantation of the custom-designed talar surface prosthesis into the predetermined position to complete reconstruction.

turn, and the superficial peroneal nerve was identified and protected during the operation. Subsequently, the joint capsule was longitudinally incised and subperiosteal dissection was performed to fully expose the distal tibial articular surface and talus fornix. The residual articular cartilage and subchondral sclerotic bone on both sides of the tibio-talar joint were completely removed by using a bone chisel, a pendulum saw, and a high-speed drill until a uniformly bloody cancellous bone bed was observed. To promote bone healing, Kirschner wires with a diameter of 2.0 mm were used to create multiple

drilling holes on the bony surface of the distal tibia and the talus apex to increase bone surface area and blood supply. After the ankle alignment was confirmed by C-arm X-ray, the internal fixator (cannulated screws, 6.5-mm diameter, Synthes, West Chester, PA, USA) was implanted. After the surgical field was thoroughly irrigated and hemostasis was achieved, the incision was sutured layer by layer.

In the replacement group, the anterior median or medial longitudinal incision of the ankle joint was made, and the skin and

APPROVED GALLEY PROOF

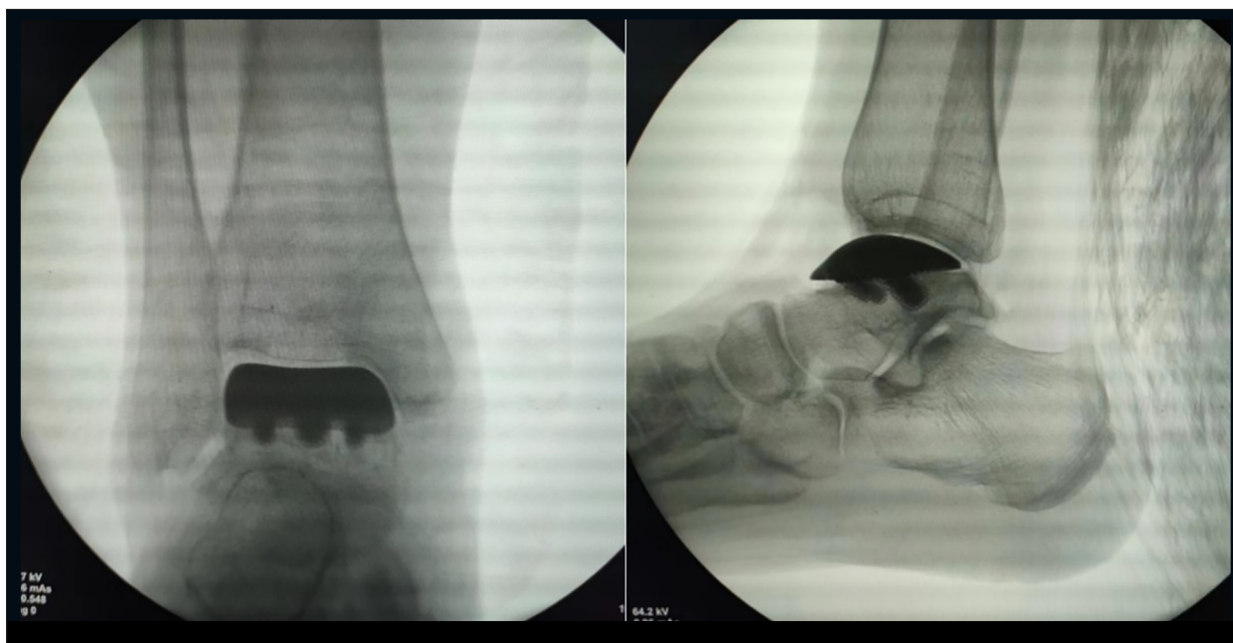


**Figure 4.** Postoperative X-ray showed that the shape and position of the talus prosthesis were acceptable, and the postoperative effect was good without obvious discomfort

subcutaneous tissue were cut in turn to expose the articular surface of the talus of the ankle joint and fully expose the lesion area of the talus. The exfoliated cartilage fragments were carefully cleaned to determine the extent of cystic degeneration. According to the preoperative 3D-printed talus model, the osteotomy guide plate was accurately placed and fixed with Kirschner wires. Then, under the guidance of the guide plate, the pendulum saw was used to perform precise osteotomy to completely remove the cystic degeneration area (Figure 3A, 3B). After removing the osteotomy guide plate, the ankle joint cavity was thoroughly cleaned and repeatedly washed with a large amount of normal saline and iodophor saline. After confirming that the joint cavity was clean, the customized 3D-printed talus prosthesis was implanted (Figure 3C, 3D). The prosthesis was secured using locking screws (Synthes, West Chester, PA, USA) with careful attention to avoid joint penetration. During the operation, a C-arm X-ray machine was used to confirm that the position of the prosthesis was satisfactory, and then screws were fixed (Figure 4). After the ankle joint was mobilized in dorsiflexion and plantarflexion to confirm the stability of the prosthesis, and the ROM and tightness of the joint were appropriate, a drainage tube was placed. Finally, the incision was sutured layer by layer and covered with a thick cotton pad combined with elastic bandage.

#### Postoperative Rehabilitation and Follow-Up

Postoperative routine fluid replacement, analgesia, anti-infection, and other symptomatic and supportive treatments were given. The drainage tube was removed according to the

drainage volume and wound exudation. After the drainage tube was removed, the patients were instructed to begin straight leg raising training, ankle pump training, and walking functional exercise. At 6 weeks after surgery, the X-ray films were reviewed, inflatable walking boots were replaced as needed, and partial weight-bearing walking training was started. The patients were followed up 12 weeks after surgery and encouraged to gradually resume normal walking activities. The X-ray films were reviewed at 6 months, 1 year, and every year after surgery, and the patients' satisfaction and functional scores were evaluated.

Clinical outcomes were assessed preoperatively and at the final follow-up (minimum 12 months) by an independent research assistant not involved in the surgical procedures. Outcome measures included (1) the AOFAS score, a 100-point clinician-administered questionnaire that evaluates pain (40 points), function (50 points), and alignment (10 points), with higher scores indicating better function; (2) the VAS, which measures pain intensity using a 10-cm horizontal line, where 0 represents no pain and 10 represents the worst imaginable pain; (3) ROM, defined as the total arc of ankle motion (dorsiflexion plus plantarflexion) measured in degrees using a standard goniometer with the patient in a seated position; (4) the SF-36, a patient-reported questionnaire that provides 2 summary scores, the Physical Component Summary and Mental Component Summary, each ranging from 0 (worst) to 100 (best); and (5) the complication rate, with all adverse events, including infection, nerve injury, prosthesis-related complications, and reoperations, recorded.

**Table 1.** Baseline characteristics of the 2 groups.

|                                | Arthrodesis group (n = 53) | Replacement group (n = 49) | P value |
|--------------------------------|----------------------------|----------------------------|---------|
| Male/female                    | 31/22                      | 28/21                      | 0.890   |
| Age, years                     | 54.85 ± 6.95               | 53.71 ± 6.29               | 0.391   |
| Left/right                     | 23/30                      | 22/27                      | 0.879   |
| Symptom duration, months       | 12.83 ± 4.44               | 12.16 ± 3.12               | 0.395   |
| Lesion area, mm <sup>2</sup>   | 250.06 ± 33.42             | 247.67 ± 40.13             | 0.745   |
| Lesion volume, mm <sup>3</sup> | 1754.02 ± 186.04           | 1749.57 ± 184.66           | 0.904   |
| Follow-up, months              | 15.72 ± 3.24               | 15.47 ± 3.16               | 0.697   |

### Statistical Analysis

Statistical analyses were performed with SPSS 26.0 (IBM Corp, Armonk, NY, USA). The Shapiro-Wilk test was used to evaluate the normality of the measured data (including VAS, AOFAS, ROM, and SF-36 scores). Data conforming to normal distribution were expressed as mean ± standard deviation. The independent-samples *t* test was used for intergroup comparison (arthrodesis group and replacement group), and the paired-samples *t* test was used for within-group comparison before and after surgery. Data that did not follow a normal distribution were presented as median (interquartile range) and analyzed with the use of nonparametric tests. Count data are expressed as the number of cases (percentage), and comparison between groups was based on sample size and theoretical frequency, using the chi-square test or Fisher exact test, as appropriate. For all statistical analyses, a *P* value of less than 0.05 was considered to indicate statistical significance.

## Results

### Comparison of General Information of the 2 Groups

A total of 102 patients (59 men and 43 women; mean age 54.3 years; age range 38-65 years) were included in the final analysis. Two patients were excluded due to insufficient follow-up duration (less than 12 months), and 1 patient was excluded owing to incomplete clinical data. As presented in **Table 1**, no statistically significant differences were observed between the 2 groups with respect to baseline characteristics, including age, sex, affected side, symptom duration, lesion extent, and follow-up period (all *P* > 0.05).

### Comparison of Ankle Joint Function Between the 2 Groups

As shown in **Table 2**, there were no statistically significant differences in baseline ankle function between the 2 patient groups prior to surgery (*P* > 0.05). Postoperative evaluations

demonstrated significant improvements in AOFAS, VAS, and ROM scores compared with preoperative measurements, with greater improvements observed in the replacement group. These differences were statistically significant (all *P* < 0.05). Notably, patients in the arthrodesis group who underwent ankle arthrodesis exhibited a near-complete loss of ankle ROM.

### Comparison of SF-36 Scores Between the 2 Groups

All patients completed the SF-36 Health Survey. As shown in **Table 3**, before surgery, there were no significant differences in the Physical Component Summary and Mental Component Summary scores between the arthrodesis group and the replacement group, ensuring comparability between the groups. The postoperative follow-up results showed that the Physical Component Summary and Mental Component Summary scores of both groups were significantly improved compared with those before surgery. However, the intergroup comparison revealed significant differences: the postoperative Physical Component Summary and Mental Component Summary scores of the replacement group were significantly higher than those of the arthrodesis group, and the differences were all statistically significant (all *P* < 0.05). This indicates that the replacement group was significantly superior to the arthrodesis group in improving the overall physical and mental health-related quality of life of patients.

### Comparison of Complications Between the 2 Groups

Postoperative complications in the 2 patient groups are summarized in **Table 4**. With regard to infection, 3 cases (5.7%) of superficial surgical site infection or impaired wound healing were observed in the arthrodesis group, compared with 2 cases (4.1%) in the replacement group. All infected cases were successfully managed through standardized wound care, antibiotic therapy, or necessary surgical debridement. Each group reported 1 case (2.0%) of transient injury to the sensory branch of the superficial peroneal nerve, manifesting as numbness in the corresponding dermatome. Symptoms in all

**Table 2.** Functional outcomes between the 2 groups.

|       |               | Arthrodesis group | Replacement group | Statistic | P value |
|-------|---------------|-------------------|-------------------|-----------|---------|
| AOFAS | Preoperative  | 66.17 ± 5.48      | 66.78 ± 1.93      | 0.643     | 0.522   |
|       | Postoperative | 78.51 ± 4.12*     | 85.88 ± 3.56*     | 9.636     | < 0.001 |
| VAS   | Preoperative  | 5.60 ± 1.26       | 5.35 ± 1.27       | 1.025     | 0.308   |
|       | Postoperative | 2.57 ± 0.87*      | 1.71 ± 0.71*      | 5.414     | < 0.001 |
| ROM   | Preoperative  | 31.74 ± 6.60      | 31.53 ± 6.01      | 0.164     | 0.870   |
|       | Postoperative | 0.91 ± 1.13*      | 48.31 ± 4.95*     | 67.787    | < 0.001 |

Note: \* Compared with preoperative results, the differences were statistically significant ( $P < 0.05$ ). Abbreviations: AOFAS, American Orthopaedic Foot and Ankle Society; VAS, visual analog scale; ROM, ankle range of motion.

**Table 3.** Comparison of SF-36 scores between the 2 groups of patients.

|                   | Physical Component Summary score |               | Mental Component Summary score |               |
|-------------------|----------------------------------|---------------|--------------------------------|---------------|
|                   | Preoperative                     | Postoperative | Preoperative                   | Postoperative |
| Arthrodesis group | 37.51 ± 5.18                     | 55.83 ± 4.96  | 51.34 ± 5.18                   | 68.15 ± 5.93  |
| Replacement group | 38.29 ± 4.96                     | 74.12 ± 4.10  | 52.90 ± 5.55                   | 78.27 ± 3.38  |
| Statistic         | 0.772                            | 20.215        | 1.467                          | 10.474        |
| P value           | 0.442                            | < 0.001       | 0.145                          | < 0.001       |

**Table 4.** Comparison of complications between the 2 groups of patients.

|                   | Infection | Nerve injury | Prosthesis-related complications | Reoperation | Total     |
|-------------------|-----------|--------------|----------------------------------|-------------|-----------|
| Arthrodesis group | 3 (5.7%)  | 1 (1.9%)     | 0 (0%)                           | 2 (3.7%)    | 6 (11.3%) |
| Replacement group | 2 (4.1%)  | 1 (2.0%)     | 1 (2.0%)                         | 0 (0%)      | 4 (8.1%)  |
| Statistic         |           |              |                                  |             | 0.287     |
| P value           |           |              |                                  |             | 0.592     |

affected patients resolved spontaneously within 3 to 6 months postoperatively. Regarding implant-related complications, no events were recorded in the arthrodesis group, whereas 1 patient (2.0%) in the replacement group exhibited a radiolucent line around the prosthesis on imaging. This finding was asymptomatic, and no specific intervention was required. In terms of reoperation rate, 2 patients (3.7%) in the arthrodesis group underwent secondary revision surgery due to failure of joint fusion, while no reoperations were documented in the replacement group. There was no statistically significant difference in overall complication rates between the 2 groups ( $\chi^2 = 0.287$ ,  $P = 0.592$ ).

## Discussion

This retrospective cohort study compared the early clinical outcomes of digitally customized 3D-printed partial talus replacement versus ankle arthrodesis in 102 patients with extensive talar necrosis. Our findings demonstrate that the 3D-printed replacement group achieved significantly superior results in functional recovery (AOFAS), pain relief (VAS), ankle joint mobility (ROM), and quality of life (SF-36), with comparable overall safety and lower reoperation rates than the arthrodesis group.

Large-scale talar necrosis is a significant therapeutic challenge in foot and ankle surgery, characterized by extensive lesion size, severe structural bone damage, and difficulty in revascularization, often leading to suboptimal outcomes with conventional

APPROVED GALLEY PROOF

joint-preserving treatments [4,11]. Currently, ankle arthrodesis is considered the gold standard for pain relief; however, this procedure entails the loss of joint mobility, which substantially compromises patients' quality of life and can lead to stress concentration and accelerated degeneration in adjacent joints [17,18]. Although total talus replacement can partially preserve joint ROM, it is associated with several challenges, including technically demanding surgical procedures, insufficient long-term prosthetic stability (eg, loosening and subsidence), polyethylene wear, and an increased risk of infection. In young, active patients, the long-term efficacy of such implants remains uncertain [19,20]. In this context, the present study incorporates digital design and 3D-printing technologies to develop patient-specific partial talar prostheses, aiming to precisely replace necrotic bone segments while maximizing preservation of healthy bone tissue and residual articular surfaces, thereby offering a novel approach to ankle joint functional reconstruction.

This study demonstrated that the replacement group exhibited a significant advantage in AOFAS scores, joint ROM, and SF-36 quality of life assessments, thereby strongly affirming the clinical value of joint-preserving surgical approaches. While traditional ankle arthrodesis effectively alleviates pain, it entails the permanent loss of joint mobility and can contribute to compensatory degeneration in adjacent joints [21,22]. In contrast, digitally designed 3D-printed partial talus prostheses enable precise reconstruction of patient-specific anatomical structures, restoring not only joint mechanical stability but also substantially improving functional performance in activities such as walking and stair climbing—aligning closely with the principles of modern “precision orthopedics” [23,24]. In recent years, the integration of 3D-printing technology into foot and ankle surgery has advanced significantly. Tracey et al [25] were the first to systematically evaluate its application in talus reconstruction, demonstrating through short-term follow-up and imaging analysis in 14 patients that the technique effectively restores collapsed talus height and achieves accurate anatomical congruence. Ando et al [26] reported favorable clinical outcomes in a 72-year-old woman 2 years after implantation of a 3D-printed ceramic total talus prosthesis. Similarly, Mu et al [27] found that following 3D-printed talus prosthesis replacement, patients' AOFAS scores improved significantly from a mean of 26.33 before surgery to 79.67 after surgery, while VAS pain scores decreased from 6.33 to 0.83. Collectively, these findings support the present study's results, indicating that 3D-printed talus prostheses offer consistent and clinically meaningful early outcomes in terms of functional recovery and pain reduction.

In terms of safety, the data from this study revealed no statistically significant difference in overall complication rates between the 2 groups, indicating that 3D-printed partial talus replacement did not introduce clinically unacceptable additional risks during the early follow-up period. Although a case

of asymptomatic radiolucent line around the prosthesis was observed in the replacement group, such imaging findings are commonly encountered in the early postoperative phase following joint reconstruction and are typically associated with interfacial bone remodeling or the development of adaptive fibrous tissue [28]. The precise clinical implications of this replacement require further clarification through long-term monitoring. Notably, a marked difference was observed in reoperation rates: 2 patients (3.7%) in the arthrodesis group underwent reoperation due to nonunion and other fusion-related failures, whereas the reoperation rate in the replacement group was zero. Nonunion following ankle arthrodesis is a well-documented and inherent risk of this procedure; therefore, this finding underscores the potential advantage of 3D-printed partial talus replacement in achieving early procedural stability.

Although digital 3D-printed partial talus replacement has demonstrated promising clinical outcomes in the early postoperative period, its long-term durability remains a primary concern within the academic community [29]. Potential long-term risks primarily include polyethylene wear under sustained mechanical loading, late-onset loosening at the prosthesis-bone interface, and degenerative changes in adjacent joints, all of which necessitate comprehensive evaluation through extended follow-up studies. Furthermore, the successful implementation of this technique relies heavily on the precise coordination of multiple sequential steps, ranging from accurate preoperative imaging and high-fidelity 3D model reconstruction to reliable metal additive manufacturing and meticulous surgical execution [30]. Any deviation in this workflow may directly compromise clinical outcomes. Moreover, current challenges include high customization costs and a prolonged prosthesis production cycle, which, to some extent, hinder the widespread adoption and clinical scalability of this technology.

This study has several limitations. First, the follow-up period was relatively short, primarily reflecting early to mid-term outcomes; the long-term prosthesis survival rate, wear characteristics, and sustained effects on adjacent joints require ongoing monitoring. Second, as a single-center study, patient recruitment and surgical procedures were conducted by a single expert team, which may limit the generalizability of the findings and underscores the need for validation through multicenter studies. Finally, although 3D-printed prostheses offer notable personalized advantages, a standardized evaluation framework remains lacking. Future efforts should focus on establishing design optimization principles and standardized imaging assessment protocols for postoperative evaluation.

## Conclusions

In early follow-up, customized 3D-printed partial talus replacement for extensive necrosis showed excellent outcomes in

preserving joint mobility, improving quality of life, and reducing reoperation rates, without increasing complications. This technique is a promising jointpreserving option for young, active patients.

### Patient Permission/Consent Declarations

Since this study is a retrospective study and the data are anonymous, consent was waived by the ethics committee.

### References:

- Parekh SG, Kadakia RJ. Avascular necrosis of the talus. *J Am Acad Orthop Surg*. 2021;29(6):e267-e78
- Cui Y, Chen B, Wang G, et al. Partial talar replacement with a novel 3D printed prosthesis. *Comput Assist Surg (Abingdon)*. 2023;28(1):21981063
- Prasarn ML, Miller AN, Dyke JP, et al. Arterial anatomy of the talus: A cadaver and gadolinium-enhanced MRI study. *Foot Ankle Int*. 2010;31(11):987-93
- Kubisa MJ, Kubisa MG, Patka K, et al. Avascular necrosis of the talus: Diagnosis, treatment, and modern reconstructive options. *Medicina (Kaunas)*. 2024;60(10):1692
- Martin Oliva X, Viladot Voegeli A. Aseptic (avascular) bone necrosis in the foot and ankle. *EFORT Open Rev*. 2020;5(10):684-90
- Gross CE, Haugom B, Chahal J, Holmes GB Jr. Treatments for avascular necrosis of the talus: A systematic review. *Foot Ankle Spec*. 2014;7(5):387-97
- Pitts C, Alexander B, Washington J, et al. Factors affecting the outcomes of tibiotalar canal fusion. *Bone Joint J*. 2020;102-B(3):345-51
- Henry JK, Rider C, Cody E, et al. Evaluating and managing the painful total ankle replacement. *Foot Ankle Int*. 2021;42(10):1347-61
- Migiorini F, Maffulli N, Baroncini A, et al. Allograft versus autograft osteochondral transplant for chondral defects of the talus: Systematic review and meta-analysis. *Am J Sports Med*. 2022;50(12):3447-55
- Hunt KJ, Ebben BJ. Management of treatment failures in osteochondral lesions of the talus. *Foot Ankle Clin*. 2022;27(2):385-99
- Scott DJ, Steele J, Fletcher A, Parekh SG. Early outcomes of 3D printed total talus arthroplasty. *Foot Ankle Spec*. 2020;13(5):372-77
- Kadakia RJ, Wixted CM, Kelly CN, et al. From patient to procedure: The process of creating a custom 3D-printed medical device for foot and ankle pathology. *Foot Ankle Spec*. 2021;14(3):271-80
- Kadakia RJ, Akoh CC, Chen J, et al. 3D printed total talus replacement for avascular necrosis of the talus. *Foot Ankle Int*. 2020;41(12):1529-36
- Fang X, Liu H, Xiong Y, et al. Total talar replacement with a novel 3D printed modular prosthesis for tumors. *Ther Clin Risk Manag*. 2018;14:1897-905
- Meng M, Wang J, Huang H, et al. 3D printing metal implants in orthopedic surgery: Methods, applications and future prospects. *J Orthop Translat*. 2023;42:94-112
- Stroud CC, Marks RM. Imaging of osteochondral lesions of the talus. *Foot Ankle Clin*. 2000;5(1):119-33
- Jeng CL, Campbell JT, Tang EY, et al. Tibiotalar canal arthrodesis with bulk femoral head allograft for salvage of large defects in the ankle. *Foot Ankle Int*. 2013;34(9):1256-66
- Ross JS, Rush SM, Todd NW, Jennings MM. Modified Blair tibiotalar arthrodesis for post-traumatic avascular necrosis of the talus: A case report. *J Foot Ankle Surg*. 2013;52(6):776-80
- Dekker TJ, Steele JR, Federer AE, et al. Use of patient-specific 3D-printed titanium implants for complex foot and ankle limb salvage, deformity correction, and arthrodesis procedures. *Foot Ankle Int*. 2018;39(8):916-21
- Cody EA, Bejarano-Pineda L, Lachman JR, et al. Risk factors for failure of total ankle arthroplasty with a minimum five years of follow-up. *Foot Ankle Int*. 2019;40(3):249-58
- Hendrickx RP, Stufkens SA, de Bruijn EE, et al. Medium- to long-term outcome of ankle arthrodesis. *Foot Ankle Int*. 2011;32(10):940-47
- Thomas R, Daniels TR, Parker K. Gait analysis and functional outcomes following ankle arthrodesis for isolated ankle arthritis. *J Bone Joint Surg Am*. 2006;88(3):526-35
- Kang Y, Park KH, Lee JW, et al. Clinical short-term analysis and effectiveness evaluation of optimally designed customized artificial talus implants. *Sci Rep*. 2025;15(1):26771
- Luo W, Zhang H, Han Q, et al. Total talar replacement with custom-made vitallium prosthesis for talar avascular necrosis. *Front Bioeng Biotechnol*. 2022;10:916334
- Tracey J, Arora D, Gross CE, Parekh SG. Custom 3D-printed total talar prostheses restore normal joint anatomy throughout the hindfoot. *Foot Ankle Spec*. 2019;12(1):39-48
- Ando Y, Yasui T, Isawa K, et al. Total talar replacement for idiopathic necrosis of the talus: a case report. *J Foot Ankle Surg*. 2016;55(6):1292-96
- Mu MD, Yang QD, Chen W, et al. Three dimension printing talar prostheses for total replacement in talar necrosis and collapse. *Int Orthop*. 2021;45(9):2313-21
- Shih CL, Chen SJ, Huang PJ. Clinical outcomes of total ankle arthroplasty versus ankle arthrodesis for the treatment of end-stage ankle arthritis in the last decade: A systematic review and meta-analysis. *J Foot Ankle Surg*. 2020;59(5):1032-39
- Park JJ, Choi JY, Lee JM, et al. Applications and effectiveness of 3D printing in various ankle surgeries: A narrative review. *Life (Basel)*. 2025;15(3):473
- Taniguchi A, Takakura Y, Tanaka Y, et al. An alumina ceramic total talar prosthesis for osteonecrosis of the talus. *J Bone Joint Surg Am*. 2015;97(16):1348-53
- Adams SB, Danilkowicz RM. Talonavicular joint-sparing 3D printed navicular replacement for osteonecrosis of the navicular. *Foot Ankle Int*. 2021;42(9):1197-20

### Declaration of Figures' Authenticity

All figures submitted have been created by the authors who confirm that the images are original with no duplication and have not been previously published in whole or in part.